

Interacting two-particle states in the symmetric phase of the chiral Nambu–Jona-Lasinio model

A. Jakovác¹ and A. Patkós¹

¹*Institute of Physics, Eötvös University, H-1117 Budapest, Hungary*

(Dated: October 6, 2022)

The renormalisation group flow of the chiral Nambu–Jona-Lasinio (NJL) model with one fermion flavor is mapped out in the symmetric phase with the help of the Functional Renormalisation Group (FRG) method using a physically motivated non-local trial effective action. The well-known infrared unstable strongly coupled fixed point characterized by a set of pointlike four-fermion couplings is reproduced. The Gaussian infrared end-point of the flow of the four-fermion couplings is now accompanied by non-zero limiting composite couplings characteristic for interacting two-particle states with finite energy and physical size. The negative interaction energy of the constituents is extracted as a function of the physical size of the composite object. This function reaches a minimum in the accessible range of physical sizes, mildly depending on the set of initial values of the couplings. The propagation of a two-particle state minimizing the interaction energy has a natural bound state interpretation.

I. INTRODUCTION

Determination of bound state spectra is of central importance in theories of fundamental interactions. The possible bound state nature of the Higgs-field is one of the actual hot questions of the physics beyond the standard model [1]. Also, low energy observables of the physics of strong interactions refer exclusively to bound states, where lattice field theory represents a most successful approach to the first principle determination of the QCD spectra [2, 3]. Considerable progress has been achieved also with this technique in the non-perturbative investigation of composite Higgs models [4].

The Bethe-Salpeter integral equation (BSE) [5, 6] is the classic "tool" of quantum field theory in solving the relativistic bound state problem. Its success depends critically on the quality of the kernel-function. Ladder-type resummations of some perturbative kernel, involving the exchange of a single force field quantum, possibly completed by additional exchange of two quanta in the crossed (t- or u-) channels, are the most frequently applied approaches. Finding the appropriate interaction vertex of the constituent field with the force field represents a further challenge. Despite of these difficulties, starting from the 1990-ies a rather systematic exploration of the mesonic and barionic bound states has been realized within the BSE-framework combined with Dyson-Schwinger equations for the quark propagators [7–10].

At about the same time was also initiated the application of the non-perturbative FRG-approach [11, 12] to the determination of bound state excitations of quantum field theories. In Ref. [13] the renormalisation group equation (RGE) of the scale-dependent four-point function $\Gamma_k^{(4)}$ has been considered. In the framework of the Wetterich-equation [11] one writes for its evolution with the scale k

$$\begin{aligned} \partial_k \Gamma_k^{(4)}(p_1, p_2, p_3, p_4) = & - \int_q \Gamma_k^{(4)}(p_1, p_2, q, -q - p_1 - p_2) \\ & \times \partial_k (G_k((p_1 + p_2 + q)^2) G_k(q^2)) \Gamma_k^{(4)}(-q, q + p_1 + p_2, p_3, p_4). \end{aligned} \quad (1)$$

Here on the right hand side only the partial k -derivative of the constituent propagators $G_k(k)$ is taken through the k -dependence of its regulator. For the bound state solution of this equation a factorized ansatz has been proposed, whose formal equivalence to the BSE has been demonstrated:

$$\Gamma_k^{(4)}(p_1, p_2, p_3, p_4) = f(p_1^2 + p_2^2, p_1^2 - p_2^2) D_k((p_1 + p_2)^2) f(p_3^2 + p_4^2, p_3^2 - p_4^2). \quad (2)$$

Here the function f stands for the bound state–constituent vertex (the Bethe-Salpeter wave function), while D_k is the propagator of the bound state composed with the two constituent fields. One expects the solution of f to display essential momentum dependence (e.g. non-local features) and D_k to produce the resonance pole when the scale pushed to the infrared limit ($k \rightarrow 0$).

A next step was the proposition for introducing a field σ representing the bound state into the effective

action by adding a quadratic form to Γ_k [14]:

$$\Gamma_k[\varphi, \sigma] = \Gamma_k[\varphi] + \frac{1}{2} O^\dagger \star \tilde{G} \star O - \sigma^\dagger \star O + \frac{1}{2} \sigma^\dagger \star \tilde{G}^{-1} \star \sigma. \quad (3)$$

The field σ couples via Yukawa-type convolution (symbolically denoted by \star) with the nonlocal field $O(q)$, formed by the constituent fields φ :

$$O(q) = \int_{p_1} \int_{p_2} g(p_1, p_2) \varphi^\dagger(-p_1) \varphi(p_2) (2\pi)^4 \delta(q - p_1 - p_2). \quad (4)$$

The strategic goal is to find the non-local Yukawa-coupling $g(p_1, p_2)$ and the propagator of the composite field \tilde{G} from the requirement that the quadratic form $\frac{1}{2} O^\dagger \star \tilde{G} \star O$ maximally cancels the resonant piece developing in Γ_k when reaching the scale characteristic for the bound state.

A rather practical "recipe" for the realisation of this strategy has been put forward in 2002 [15]. A composite field was introduced into the original action by replacing the pointlike four-fermion interaction by a pointlike Yukawa interaction with the bound state field using a local Hubbard-Stratonovich (HS-) transformation [16, 17]. On the example of a gauged chiral NJL model with one fermion species the authors have demonstrated the existence of two (partial) fixed points connected along a one dimensional "renormalized trajectory" following the variation of the effective four-fermion coupling. The neighbourhood of the infrared unstable fixed point represents a strongly coupled interactive theory, which describes via the HS-transformation the dynamics of an elementary scalar field. The other, infrared stable fixed point corresponds to the electrodynamics of massless fermions. It was conjectured that during its evolution towards the infrared the scalar field transmutes into the representative of the positronium-like fermion-antifermion bound state. Although this last conjecture has not been confirmed explicitly, since then the extension of any effective theory with fields representing composite (bound) objects with appropriate quantum numbers has become a common usage. The generalisation of the local HS-transformation to larger sets of composite fields has been worked out [18, 19] and important steps were made towards the application of this FRG-technique to n -point functions of QCD [20].

The basic steps of the procedure called "dynamic hadronisation" [21–23] can be summarized as follows: The composite local field is constructed from the constituent fields with an arbitrary three-variable weight function. Its scale dependence is deduced from the "no-run" requirement enforced on the 4-fermion couplings. Therefore the three-point function has no direct contact to the Bethe-Salpeter wave function of the two-particle composite. The usual initial condition for the RG-equations consists of setting 4-fermion couplings equal to zero at the cut-off. Is this physical? Can one start at a scale where already no individual fermions, but only correlated fermion pairs do interact? Although the mapping of the 4-fermion theory on the Yukawa-type theory with such a supplementary requirement is in principle exact, but its adequacy is questionable when only a subset of the operators is included into the renormalisation flow.

Another sort of intriguing question is related to the set of composite fields. Can one rely on a unique field representing the complete spectra in a given channel? A careful detailed FRG-analysis of the full s-channel spectra provides evidence for a negative answer to this question, using the example of QED [24]. What concerns strong interactions, the lowest meson masses might be satisfactorily fitted within a quark-meson effective model with pointlike Yukawa terms [25–27]. Despite of this fact, at present we do not know if the s-channel singularity structure of the 4-fermion function consistently reproduces them.

We propose to return to the investigation of non-local extensions of the effective action [14]. We follow a slightly different strategy and shall concentrate on the renormalisation flow in an extended coupling space towards the infrared. The set of couplings contains those which one suspects intuitively to signal bound state formation. In particular, the scale evolution of the composite-2fermion vertex function (Yukawa-coupling) will be determined dynamically, not by a constraint equation. Since the resonant state cannot exhaust the spectral function of a certain channel, we trace also the evolution of the pointlike 4-fermion vertices towards zero, as expected from the simplified RG-analysis. They fade away in the neighbourhood of the IR fixed point.

The numerical solution starts in the ultraviolet regime (much above the characteristic momentum scale of the composite state) from the neighbourhood of the ultraviolet fixed point [28] characterized by a non-vanishing set of 4-fermion couplings. It will be argued that along some unstable directions the system enters the regime with non-zero Yukawa coupling describing the association of two fermions into a bosonic composite and also a non-zero pointlike 4-point function of the composites.

One reaches very quickly a scaling regime for the dimensional couplings. One finds that the Gaussian

fixed point is the only IR stable fixed point in the subspace of the pointlike fermionic couplings as it is the case of the 4-fermion NJL theory [28]. In particular, the strength of the constituent-composite 3-point function tends logarithmically to zero as well as the four-boson coupling. The truly new feature is that along the trajectories passing in the subspace of the dimensionful composite couplings one observes the existence of a sequence of limiting finite masses and composite object sizes, corresponding to interacting two-particle states of different physical size and well defined interaction energy.

The structure of this paper is the following. In section 2 we extend the effective action of the model with the contributions reflecting the presence of two-particle states composed from two fermions. Via a non-local Hubbard-Stratonovich transformation we arrive at the form of the effective action for which the RG-equations are formulated in section 3. In section 4 the features of the RG flow are analyzed numerically and interpreted in favor of the existence of a bound state in the symmetric phase.

II. THE MODEL AND ITS PHYSICALLY MOTIVATED EFFECTIVE ACTION ANSATZ

The Fierz complete defining action of the one-flavor chiral NJL-model is the following:

$$\Gamma_{NJL} = \int d^4x \left[i\bar{\psi}\gamma_m\partial_m\psi + 2\lambda_\sigma (\bar{\psi}_L\psi_R)(\bar{\psi}_R\psi_L) - \frac{1}{2}\lambda_V(\bar{\psi}\gamma_m\psi)^2 \right]. \quad (5)$$

We shall investigate the emergence of a bound state in the scalar-pseudoscalar channel by explicitly introducing into the scale dependent effective action a four-point term which describes the propagation of a non-local composite two-particle operator in the s -channel. One still keeps non-resonating pointlike four-fermion interactions with strength $\delta\lambda_\sigma, \lambda_V$:

$$\begin{aligned} \Gamma_{NL-NJL} = & \int d^4x \left[\bar{\psi}i\gamma_m\partial_m\psi - \frac{1}{2}\lambda_V(\bar{\psi}\gamma_m\psi)^2 + 2\delta\lambda_\sigma(\bar{\psi}_R\psi_L)(\bar{\psi}_L\psi_R) \right] \\ & + 2 \int d^4x \int d^4y \int d^4x_1 \int d^4x_2 \int d^4y_1 \int d^4y_2 \\ & \times \bar{\psi}_R(x_1)\bar{\psi}_L(x_2)\Delta_C(x-x_1, x-x_2)G_C(x-y)\Delta_C(y-y_1, y-y_2)\bar{\psi}_L(y_1)\psi_R(y_2). \end{aligned} \quad (6)$$

The binding function $\Delta_C(x-x_1, x-x_2)$ propagates the $U_A(1) \times U_V(1)$ (globally) invariant fermion and anti-fermion elementary fields from the location (x_1, x_2) to the location x of the composite. The propagation of the composite field is accounted by the propagator $G_C(x-y)$. Both functions have to be determined dynamically.

One can easily construct a non-local Hubbard-Stratonovich transform introducing the auxiliary scalar $\Phi_S(x)$ and pseudoscalar $\Phi_5(x)$ fields with the following correspondence to nonlocal composites:

$$\begin{aligned} \Phi_S(y) & \leftrightarrow i \int dx \int dx_1 \int dx_2 G_C(y-x)\Delta_C(x-x_1, x-x_2)\bar{\psi}(x_1)\psi(x_2), \\ \Phi_5(y) & \leftrightarrow \int dx \int dx_1 \int dx_2 G_C(y-x)\Delta_C(x-x_1, x-x_2)\bar{\psi}(x_1)\gamma_5\psi(x_2). \end{aligned} \quad (7)$$

If one also adds to the effective action a local potential term which is fourth power in the composite fields, then one has

$$\begin{aligned} \Gamma_{NL-NJL} = & \int d^4x \left[\bar{\psi}i\gamma_m\partial_m\psi - \frac{1}{2}\lambda_V(\bar{\psi}\gamma_m\psi)^2 + 2\delta\lambda_\sigma(\bar{\psi}_R\psi_L)(\bar{\psi}_L\psi_R) + \frac{\lambda}{24}(\Phi_S^2(x) + \Phi_5^2(x))^2 \right] \\ & + \frac{1}{2} \int dx \int dy \left[\Phi_S(x)\Gamma_C^{(2)}(x-y)\Phi_S(y) + \Phi_5(x)\Gamma_C^{(2)}(x-y)\Phi_5(y) \right] \\ & - i \int dx \int dx_1 \int dx_2 \Delta_C(x-x_1, x-x_2) \left[\Phi_S(x)\bar{\psi}(x_1)\psi(x_2) - i\Phi_5(x)\bar{\psi}(x_1)\gamma_5\psi(x_2) \right]. \end{aligned} \quad (8)$$

The two-point function of Φ_S and Φ_5 is the same inverse function of the chiral propagator:

$$\int dz G_C(x-y)\Gamma_C^{(2)}(y-z) = \delta(x-z). \quad (9)$$

In the symmetric phase the scalar and the pseudoscalar spectra are degenerate. We shall use a simplified one-particle form:

$$\Gamma_S^{(2)}(q) = Z_C q^2 + M_C^2 = \Gamma_5^{(2)}(q). \quad (10)$$

By the above construction this analytic structure shows up also in the four-fermion function. If the RG-equations display a set of solutions characterized by a continuous variation of the limiting IR-value of M_C^2 then this ansatz corresponds rather to a certain (imperfect) description of the two-particle continuum, than to some real bound state. A bound state might be signaled by the existence of well distinguishable minima in the effective squared "mass". The concept will be elaborated more accurately below in the main text.

The other quantity which needs explicit modeling is the 3-point bosonic composite-fermion-fermion function. The simplest parametrisation used in a first investigation is to assume a Gaussian shape both in the center-of-mass momentum of the composite and in the relative momentum of the two fermion constituents:

$$\Delta_C(q_1, q_2) = g_C e^{-\beta(q_1+q_2-Q)^2} e^{-\alpha(q_1-q_2)^2}, \quad (11)$$

with scale dependent parameters g_C, β, α . For the sake of reducing the dimension of the coupling space the widths of the two Gaussians are assumed to be equal: $\beta = \alpha$. The parameter α can be interpreted as the square of the physical size of the two-particle state, $\alpha \sim R_{phys}^2$. Its scale dependence will be investigated with RG-equations. It will be shown that for a decreasing series of its initial values defined at the maximum scale Λ , for each of them a well-defined limiting behavior is obtained in the infrared. The IR-value of the squared propagator mass M_C^2 depends on the infrared size of the system and on one additional renormalisation condition to be specified in section IV. Since it varies also continuously, one is tempted to conclude that our trial effective action actually represents a continuous set of two-particle states. The question is if some specific characterisation could still suggest bound state formation. There an affirmative answer will be claimed to this question.

In the next section, the Wetterich-equations will be deduced for the couplings $\delta\lambda_\sigma, \lambda_V, g_C, \alpha, M_C, \lambda$ with a general regulator function.

III. THE RENORMALISATION GROUP EQUATIONS

It is convenient to split the right hand side of the Wetterich equation [11, 12] into three pieces:

$$\partial_t \Gamma = -\text{Tr} \log \Gamma_F^{(2)} + \frac{1}{2} \text{Tr} \log \Gamma_B^{(2)} + \frac{1}{2} \text{Tr} \log (I - G_B \Gamma_{BF}^{(2)} G_F \Gamma_{FB}^{(2)}). \quad (12)$$

where $\Gamma^{(2)}$ refers to the second functional derivative matrix of the effective action, $\Gamma_{B/F}^{(2)}$ represents the purely bosonic/fermionic derivative matrix, while the mixed matrices are denoted by $\Gamma_{BF}^{(2)}$ or $\Gamma_{FB}^{(2)}$. The variable $t = \ln(k/\Lambda)$ relates the actual scale k to the initial (cut-off) scale Λ .

The first term on the right hand side can be rewritten with the help of the massless fermion propagator $G_\psi^{(0)}$:

$$-\text{Tr} \log \Gamma_F^{(2)} = -\text{Tr} \log \Gamma_F^{(2)}(m_\psi = 0) - \text{Tr} \log (I + G_\psi^{(0)} \Delta \Gamma_{\bar{\psi}\psi}). \quad (13)$$

The quantity $\Delta \Gamma_{\bar{\psi}\psi}$ is independent of the fermi-fields, and depends linearly on the composite fields. Therefore its second derivative contributes a fermion-bubble to the RGE of the composite two-point function and its fourth derivative to the running of the pointlike quartic composite coupling (the fermion quadrangle).

The purely bosonic contribution on the right hand side of (12) has the following explicit form on constant composite field background:

$$\frac{1}{2} \text{Tr} \log \Gamma_B^{(2)} = \frac{1}{2} \int_q \log \left[\left(\Gamma_S + \frac{\lambda}{2} \Phi_S^2 + \frac{\lambda}{6} \Phi_5^2 \right) \left(\Gamma_5 + \frac{\lambda}{2} \Phi_5^2 + \frac{\lambda}{6} \Phi_S^2 \right) - \frac{\lambda^2}{9} \Phi_S^2 \right]. \quad (14)$$

The second derivative with respect to Φ_S gives a tadpole contribution to the RGE of M_C^2 . Since the tadpole is momentum independent, it does not contribute to the field renormalisation. Therefore there is no need to consider the pure bosonic term in non-constant background. The fourth derivative gives the composite one-loop contribution to the running of itself.

The RG-equation of the composite scalar two-point function is as follows:

$$\partial_t \Gamma_S^{(2)}(P) = \int_q \left[-\Delta_C(q, -q - P) \Delta_C(-P + q, q) \hat{\partial}_t \text{Tr}_D G_\psi^{(0)}(q) G_\psi^{(0)}(q - P) + \frac{\lambda}{2} \hat{\partial}_t \left(G_S(q) + \frac{1}{3} G_5(q) \right) \right]. \quad (15)$$

The RG-equation of M_C^2 is arrived by setting $P = 0$ on both sides, while $\eta_C = -\partial_t \ln Z_C$ is found by taking first the second derivative $\partial^2 \Gamma_S^{(2)}(P) / \partial P_m^2$ and setting $P = 0$ in the derivative.

The RGE of λ is the sum of the pure composite and the pure fermion loop:

$$\hat{\partial}_t \lambda = 24 \int_q \hat{\partial}_t \frac{1}{Z_\psi^4 (1 + r_F(q))^4 q^4} \Delta_C^2(q, -q) \Delta_C^2(-q, q) - \frac{3\lambda^2}{2} \int_q \hat{\partial}_t \left(G_S^2(q) + \frac{1}{9} G_5^2(q) \right). \quad (16)$$

Since one needs the anomalous scaling of the fermion propagator, also the expression of the fermionic self-energy contribution is found from the third term of (12), when the logarithm is expanded to linear power:

$$\partial_t \Gamma_\psi^{(2)}(P) = \frac{1}{2} \int_q \Delta_C(P, q - P) \Delta_C(-q + P, -P) \hat{\partial}_t \left[(G_S(q) + G_5(q)) G_\psi^{(0)}(q - P) \right]. \quad (17)$$

There are two contributions to the composite boson - fermion - fermion three-point function. In the first the fermion legs interact via t-channel exchange of the composite field itself, in the second a fermion loop is generated by taking into account the four-fermion interactions:

$$\begin{aligned} & \partial_t \Gamma_{\bar{\psi}\psi S}^{(3)}(P_1, P_2, P_3) \\ &= \frac{1}{8} \int_q \Delta_C(P_1, q - P_1) \Delta_C(P_1 - q, q + P_2) \Delta_C(-q - P_2, P_2) \hat{\partial}_t \left[\text{tr}_D G_\psi^{(0)}(q - P_1) G_\psi^{(0)}(q + P_2) (G_5(q) - G_S(q)) \right] \\ &+ (\delta\lambda_\sigma + \lambda_V) \int_q \Delta_C(-P_3 - q, q) \hat{\partial}_t \left(\text{tr}_D G_\psi^{(0)}(q) G_\psi^{(0)}(q + P_3) \right). \end{aligned} \quad (18)$$

The RG-equation of the strength g_C is determined by setting all external momenta zero. The running of the width α of the composite "wave function" is determined first setting $P_1 = P_2 = -P_3/2 \equiv -P/2$, next taking the second derivative with respect to P_m on both sides and eventually setting $P = 0$.

Finally, we need the RG-equations of the two-types of pointlike four-fermion couplings. One has three contributions all coming from the third term on the right hand side of (12). The exchange of two composite mesons gives

$$\begin{aligned} & -\frac{1}{16} \hat{\partial}_t \int_q \frac{\Delta_C^2(q, 0) \Delta_C^2(-q, 0)}{Z_\psi^2 (1 + r_F(q))^2 q^2} [(G_S^2(q) + G_5^2(q)) (\bar{\psi} \gamma_m \psi)^2 + 2G_S(q) G_5(q) (\bar{\psi} \gamma_m \gamma_5 \psi)^2] \\ &= -\frac{1}{16} \hat{\partial}_t \int_q \frac{\Delta_C^2(q, 0) \Delta_C^2(-q, 0)}{Z_\psi^2 (1 + r_F(q))^2 q^2} [(G_S(q) + G_5(q))^2 (\bar{\psi} \gamma_m \psi)^2 + 4G_S(q) G_5(q) ((\bar{\psi} \psi)^2 - (\bar{\psi} \gamma_5 \psi)^2)] \end{aligned} \quad (19)$$

The second equality is arrived at after exploiting Fierz-identity $(\bar{\psi} \gamma_m \gamma_5 \psi)^2 = 2((\bar{\psi} \psi)^2 - (\bar{\psi} \gamma_5 \psi)^2) + (\bar{\psi} \gamma_m \psi)^2$.

The second contribution comes from combining the exchange of one composite boson and the pointlike (non-resonant) four-fermion interaction:

$$\begin{aligned} & \frac{1}{4} \hat{\partial}_t \int_q \frac{\Delta_C(0, q) \Delta_C(0, -q)}{Z_\psi^2 (1 + r_F(q))^2 q^2} \\ & \times \left[((\bar{\psi} \psi)^2 + (\bar{\psi} \gamma_5 \psi)^2) (G_S(q) - G_5(q)) (-2\delta\lambda_\sigma + \lambda_V) \right. \\ & + ((\bar{\psi} \psi)^2 - (\bar{\psi} \gamma_5 \psi)^2) (G_S(q) + G_5(q)) (-\delta\lambda_\sigma + \lambda_V) \\ & \left. - (\bar{\psi} \gamma_m \psi)^2 (G_S(q) + G_5(q)) (\delta\lambda_\sigma + \lambda_V) \right]. \end{aligned} \quad (20)$$

It is clear that the explicit symmetry breaking in the boson propagators would induce symmetry breaking in the four-fermion couplings. In the following we shall substitute here and in all RG-equations $G_s(q) = G_5(q)$.

The third contribution comes from the fermion bubble of the nonresonant fermion-fermion scattering which formally coincides with FRG contributions of the original NJL model:

$$-\hat{\partial}_t \int_q \frac{2}{Z_\psi^2 (1 + r_F(q))^2 q^2} \left((\bar{\psi}\psi)^2 - (\bar{\psi}\gamma_5\psi)^2 \right) (\delta\lambda_\sigma^2 + 4\delta\lambda_\sigma\lambda_V + 3\lambda_V^2) + \frac{1}{2} (\bar{\psi}\gamma_m\psi)^2 (\lambda_V^2 + 2\delta\lambda_\sigma\lambda_V + \delta\lambda_\sigma^2) \right). \quad (21)$$

This expression leads to the RGE of the NJL theory with Fierz-complete pointlike couplings [28].

The explicit equations of the RG-flow with specific regulator function choice appear in the Appendix.

IV. RG-FLOW NEAR THE FIXED POINT SOLUTIONS

The extended set of RG-equations in the Appendix admits the same two fixed points like the 4-fermion model with pointlike couplings. Below we shall characterize the behavior of complete set of couplings in their respective neighbourhood (for the definitions of the dimensionless couplings, see (40) in the Appendix).

The fixed points of the Fierz-complete chiral symmetric NJL-model (with all bosonic couplings set zero) are well-known [28, 30]. The flow-equations for the rescaled dimensionless 4-fermion couplings (see Appendix) read as

$$\begin{aligned} \partial_t \delta\lambda_{\sigma r} &= 2\delta\lambda_{\sigma r} - \frac{1}{8\pi^2} (\delta\lambda_{\sigma r}^2 + 4\delta\lambda_{\sigma r}\lambda_{Vr} + 3\lambda_{Vr}^2), \\ \partial_t \lambda_{Vr} &= 2\lambda_{Vr} - \frac{1}{16\pi^2} (\delta\lambda_{\sigma r} + \lambda_{Vr})^2 \end{aligned} \quad (22)$$

have three fixed points: the IR-attractive trivial

$$(\delta\lambda_{\sigma r}^*, \lambda_{Vr}^*) = (0, 0) \quad (23)$$

the partially UV-repulsive, strongly interacting and stable

$$(\delta\lambda_{\sigma r}^*, \lambda_{Vr}^*) = (6\pi^2, 2\pi^2), \quad (24)$$

and the partially UV-repulsive, strongly interacting and unstable

$$(\delta\lambda_{\sigma r}^*, \lambda_{Vr}^*) = (-64\pi^2, 32\pi^2). \quad (25)$$

The Gaussian fixed point is absolute infrared attractive, the other two have one attractive and one repulsive direction.

A. The strongly coupled IR-unstable fixed point

In the framework of the extended effective action we investigate the behaviour of the composite bosonic couplings around the fixed point (24). Since the anomalous dimensions η_C, η_ψ are both proportional to \tilde{g}_{Cr}^2 they can be neglected in the equation of \tilde{g}_{Cr}^2 , which arises from linearizing (43) around the fermionic fixed point:

$$\partial_t \tilde{g}_{Cr}^2 \approx -(\delta\lambda_{\sigma r}^* + \lambda_{Vr}^*) \frac{2F_1(0)}{\pi} \tilde{g}_{Cr}^2 = -4\pi \tilde{g}_{Cr}^2, \quad (26)$$

with the solution

$$\tilde{g}_{Cr}^2 \left(\frac{k}{\Lambda} \right)^{4\pi} = 1 \quad (27)$$

(in the stability analysis we set $\alpha_r = 0$). This means that the Yukawa-coupling is IR-relevant around this fixed point.

One notes that as a (small) non-zero initial value of the Yukawa coupling starts to grow around this

fixed point, it induces an increase of μ_C^2 . The linear part of (45) can be written in this regime as

$$\partial_t \mu_C^2 = -2\mu_C^2 + \frac{1}{4\pi^2} \tilde{g}_{Cr}^2 \quad (28)$$

which in addition to the solution of the homogeneous equation suggests the following proportionality

$$\mu_C^{(inh)^2}(t) = A \tilde{g}_{Cr}^2(t). \quad (29)$$

With the coefficient

$$A = \frac{1}{8\pi^2(1-2\pi)} \quad (30)$$

one finds for the solution

$$\mu_C^2(t) = \mu_C^2(t=0) \left[1 + \frac{\mu_C^{-2}(t=0)}{8\pi^2(1-2\pi)} \right]^{-1} \left[\left(\frac{k}{\Lambda} \right)^{-2} + \frac{\mu_C^{-2}(t=0)}{8\pi^2(1-2\pi)} \left(\frac{k}{\Lambda} \right)^{-4\pi} \right]. \quad (31)$$

The four-boson coupling stays zero at linear order (see (46)!). The width of the bosonic wave-function follows the leading order equation (the second equation of (43))

$$\partial_t (\tilde{g}_{Cr} \alpha_r) = 2\tilde{g}_{Cr} \alpha_r - \frac{\tilde{g}_{Cr}}{2}, \quad (32)$$

which implies that $g_{Cr} \alpha_r \sim B g_{Cr}$, if it starts with zero at $t = 0$. After substitution one finds

$$\alpha_r = \frac{1}{4(1+\pi)}, \quad (33)$$

which means in physical units a quadratically increasing value with k . The scaled value is rather small, confirming the selfconsistency of evaluating $F_n(\# \alpha_r), H_n(\# \alpha_r)$ at $\alpha_r = 0$.

One can conclude that the fixed point (24) is fully IR-unstable also along the directions of the composite couplings.

B. Analytic features of the mass-distorted Gaussian fixed point

Assuming first $\eta_C, \eta_\psi \approx 0$, one instantly finds that the irrelevant nature of the dimensionless pointlike 4-fermion couplings $\delta\lambda_{\sigma r}$ and λ_{Vr} is unchanged, and similarly $\alpha_r \rightarrow 0$ for $k \rightarrow 0$. The rescaled μ_C^2 increases as $\sim k^{-2}$ and its physical value M_C^2 remains close to its initial value, only slightly modified due to the interactions.

In the neighbourhood of the Gaussian fixed point, when the system is driven below the mass scales the RG-flow of \tilde{g}_{Cr}^2 is understood with the help of the approximate expression of η_C (η_ψ becomes very quickly negligible and $\alpha_r \approx 0$ is also a very good approximation):

$$\partial_t \tilde{g}_{Cr}^2 \approx \eta_C \tilde{g}_{Cr}^2, \quad \eta_C \approx \frac{\tilde{g}_{Cr}^2}{4\pi^2}, \quad (34)$$

which leads to the following IR-behavior when starting the solution at $k = k_0$:

$$\tilde{g}_{Cr}^2(k) = \frac{\tilde{g}_{Cr}^2(k_0)}{1 + \frac{\tilde{g}_{Cr}^2(k_0)}{4\pi^2} \ln \frac{k_0}{k}}. \quad (35)$$

It is logarithmically approaching zero, independently of the initial coupling. We could check that the variation of \tilde{g}_{Cr}^2 found numerically (see next subsection) indeed follows this behavior and also $\tilde{g}_{Cr}^2(t)$ is proportional to $\eta_C(t)$. In this way, the anomalous fermionic and bosonic dimensions are both negligible in the immediate neighborhood of the fixed point.

The asymptotic flow of λ_r is governed by the following approximate equation, after the composite

bubble diagram is stopped to contribute by the increase of μ_C^2

$$\partial_t \lambda_r \approx \frac{\tilde{g}_{Cr}^2}{2\pi^2} \lambda_r - \frac{3\tilde{g}_{Cr}^4}{\pi^2}. \quad (36)$$

The second term is negligible for $|t| \rightarrow \infty$ and substituting the extreme asymptotic from of (35) one arrives at

$$\lambda_r(t) \approx |t|^{-2}. \quad (37)$$

C. Detailed numerical study of the flow near the Gaussian fixed point

The RG flow was studied around the Gaussian fixed point numerically. Our intention was to set the initial values of the couplings at "macroscopic" distance from the Gaussian fixed point, though much closer than to the strongly coupled fixed point. A major question arises concerning the number of freely allowed initial choices among the dimensionful parameters.

The starting value of $\alpha(t=0) \sim R_{phys}^2(t=0)$ controls the initial size of the system. Very large values (e.g. $\alpha_r = 100 - 1000$) correspond essentially to uniform spatial distribution of the constituents. In this limiting case the effect of the quantum fluctuations on M_C^2 should be interpreted as the sum of the self-energies of the separate constituents. One expects that the initial contributions (from the far ultraviolet) should follow the same t -dependence when $\alpha_r(0)$ is lowered. This is expressed by the following renormalisation condition:

$$\frac{dM_C^2}{dt}(\alpha_r^{(1)}(0), \mu_C^{2(1)}(0)) = \frac{dM_C^2}{dt}(\alpha_r^{(2)}(0), \mu_C^{2(2)}(0)). \quad (38)$$

Whenever one fixes the first pair containing a large value of $\alpha_r^{(1)}(0)$ then for the next (lower) $\alpha_r^{(2)}(0)$ value the corresponding initial value of $\mu_C^{2(2)}$ should be found by solving the above equation.

This procedure seems to be somewhat arbitrary. We argue that through this renormalisation condition we are able to introduce some physical features of the two-particle state which cannot be built in explicitly into the assumed oversimplified form of the composite two-point function.

A generic "reference" run has been started with the initial conditions $\alpha_r(0) = 100$, $\mu_C^2(0) = 0.5$, $\lambda_r(0) = 10$, $g_{Cr}^2(0) = 10$, $Q_r^2(0) = 1$, $\delta\lambda_{\sigma r}(0) = 1$, $\lambda_{Vr}(0) = 1$. Keeping all other initial values fixed, a lowered choice $\alpha_r(0) = 1.5$ requires by (38) $\mu_C^2(0) = 0.37$, meaning that the initial value of μ_C^2 varies rather slowly under the variation of the initial size. For each set we start at $t = 0$ and follow the evolution to $t = -10$ (restricted by the numerical stability of the applied Mathematica procedure). This is more than sufficient to recognize the asymptotic tendencies in all couplings for $k \rightarrow 0$.

The features of the RG-flow for the representative set of the initial parameters can be summarized as follows.

- First peek in the dimensionless quantities. If we plot the rescaled Yukawa coupling $Z_C \tilde{g}_{Cr}^2$ after a transient increase a clear constant asymptotics is seen (see the left figure of FIG.1). This is consistent with and indirectly checks numerically the validity of both asymptotic equations in (34). Concerning the scalar self-coupling λ_r , we can observe only a very slow variation (see the right figure of FIG.1), making hard to draw any quantitative conclusion on its compatibility with the limiting behavior (37).
- The anomalous dimension of the composite scalar field converges to zero as displayed in FIG.2 and in quantitative agreement with the expectation based on the estimated asymptotics in (34). The anomalous dimension of the fermi-field stays very small from the very start of the RG-evolution.
- The 4-fermion couplings are, by their physical dimension, irrelevant in the IR around the Gaussian fixed point. By rescaling with the canonical dimension we find an almost constant behavior (see FIG. 3). We remark that starting with too large values for these couplings would drive the solution of the RG-equations to instability.
- Other dimensionful quantities are M_C^2 and α . We plot in FIG. 4 the physical value of M_C^2 and the dimensionless combination αM_C^2 . As it can be seen from the figures, both quantities converge very quickly to their asymptotic nonzero values. If one fixes the value of $M_C^2(k=0)$ to some value in

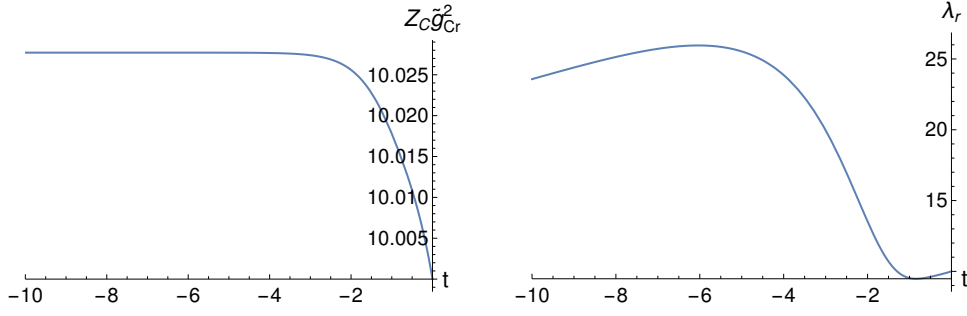


FIG. 1. RG-evolution of the rescaled composite-to-constituents Yukawa coupling and the four-boson interaction vertex coupling

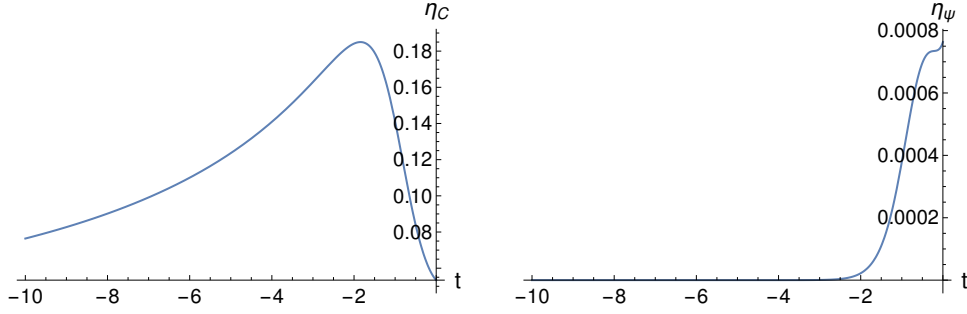


FIG. 2. RG-variation of the anomalous dimension η_C demonstrates the evolution of the composite field towards the canonical kinetic term.

GeV^2 then the physical size $R_{phys}^2(k=0)$ is determined by the asymptotics as a well-defined value in GeV^{-2} .

- Next, we explore the behavior of the effect of quantum fluctuations on the squared mass parameter by displaying $\delta M_C^2(\alpha(k=\Lambda)) \equiv M_C^2(k=0, \alpha(k=\Lambda)) - M_C^2(k=\Lambda, \alpha(k=\Lambda))$ as a function of t for gradually decreasing values of $\alpha(k=\Lambda)$ (accompanied by the corresponding choice of $\mu_C^2(0)$). In FIG. 5 one notices the equal slope starting rise (required by the renormalisation condition) is followed by a drop which gets apparently larger as $\alpha_r(k=\Lambda)$ is lowered. The decrease in $\delta M_C^2(\alpha(k=\Lambda))$ relative to the case of the completely unbound particles ($\alpha_r(k=\Lambda) \approx \infty$) lends itself to a physical identification with an attractive interaction energy.
- One can display the interaction energies $\Delta M_C^2 \equiv \delta M_C^2(\alpha(k=\Lambda)) - \delta M_C^2(\alpha(k=\Lambda) = \infty)$ and the squared physical size $\alpha(t=-\infty)$ as functions of the initial squared physical size $\alpha(k=\Lambda)$. By the

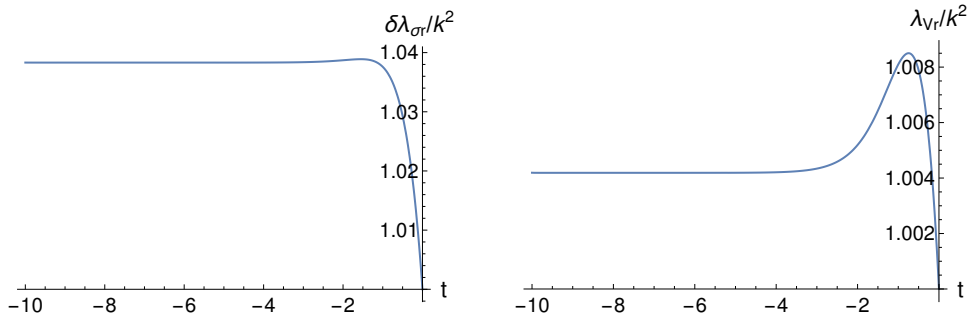


FIG. 3. RG evolution of the rescaled 4-fermion couplings.

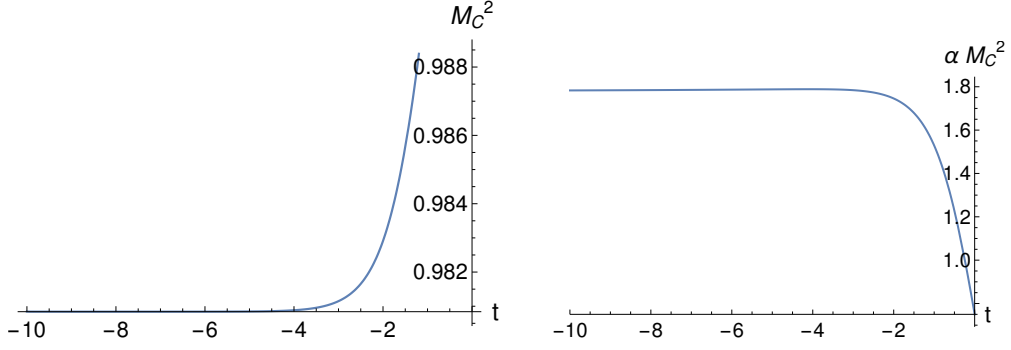


FIG. 4. RG-variation of the squared boson mass and of the width of the composite "wave function".

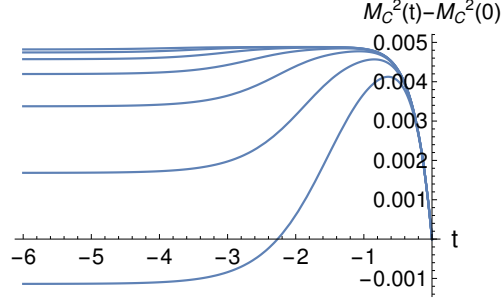


FIG. 5. RG-variation of the quantum contribution to the squared composite mass $\delta M_C^2(\alpha(k = \Lambda)) = M_C^2(t = -\infty, \alpha(k = \Lambda)) - M_C^2(t = 0, \alpha(k = \Lambda))$. From the top to the bottom curves with diminishing $\alpha_r(k = \Lambda)$ are presented.

previous figure a sequence of monotonically increasing (less and less negative) interaction energy function is expected with increasing $\alpha(t = 0)$. But, in the range $2.5 > \alpha(t = 0) > 1.0$ an opposite tendency takes over (see FIG. 6), leading to a minimum in the dependence of the interaction energy on the initial size of the two-particle composite. Similar behaviour is observed in $\alpha(t = -\infty)$ as a function of the initial size. In the figure on the right one notices that quantum fluctuations diminish the final size for large initial values, but it gets larger than the initial value if one "squeezes" it beyond a certain size. The minimum of the final size qualitatively coincides with the maximum of the negative interaction energy. When states are compared along a different initial slope dM_C^2/dt the locations of the minima are shifted in a correlated way and also the minimal values change mildly. The most natural conclusion is that the composite which corresponds to the minimum

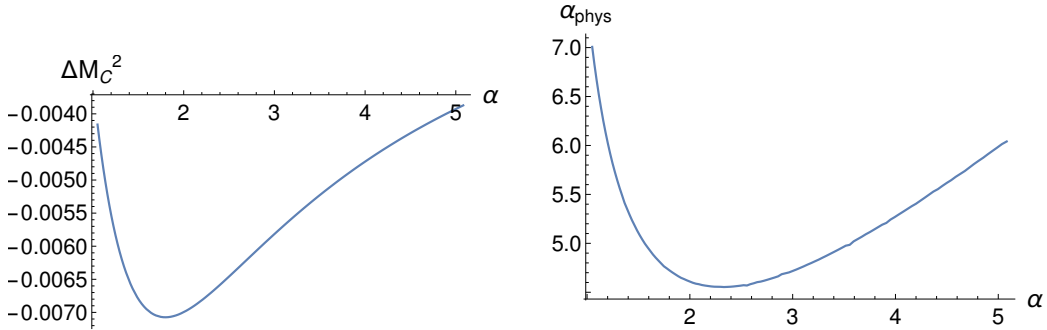


FIG. 6. Dependence of the interaction energy and of the squared physical size of the composite on the cut-off value of the size parameter

(negative maximum) of the interaction energy is a stable configuration, in other words it is natural

to interpret it as a bound state.

It is worthwhile to observe the following mapping among the "potentials" derived with different starting dM_C^2/dt . In the left figure of FIG.7 a set of the potentials is shown for which this derivative has been fixed by choosing at $\alpha(t=0) = 1000$ the values $\mu_C^2(t=0) = 0.08, 0.1, 0.2, \dots, 1.2$, respectively. Using (38) for each of them one finds the corresponding $\alpha(t=0), \mu_C^2(t=0)$ values and in the same steps as for FIG.6 one constructs the interaction energy vs. initial squared size curve. The smooth deformation due to the change of the initial data allows to map the potentials onto each other (figure on the right). The multiplicative scaling of ΔM_C^2 compensates is fixed by the requirement $\Delta M_{Cmin}^2/C = -1$. Then the coefficients of the linear mapping of the α -scale $\alpha \rightarrow A_1\alpha + A_2$ are determined completely by fixing the location of the maximally negative interaction energy to $A_1\alpha_{min} + A_2 = 1$, which leads to

$$A_i = q_{1i}C + q_{2i} + q_{3i}\sqrt{C}. \quad (39)$$

In this way the size of the two-particle system with maximally negative interaction energy is determined by the maximal interaction energy (binding energy) itself. The whole curve is now parametrized with the help of $|\Delta M_C^2|_{max}$.

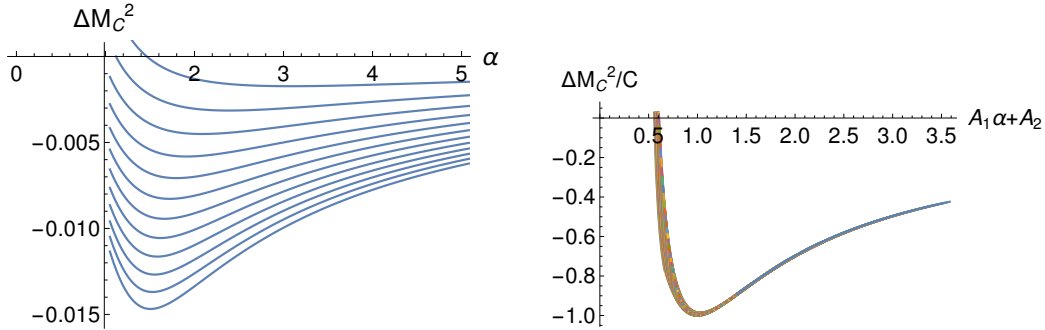


FIG. 7. Left: Dependence of the interaction energy on the input value of the size parameter, for different dM_C^2/dt at $t=0$, Right: the set of potentials scaled together with the mapping $M_C^2 \rightarrow M_C^2/C, \alpha(k=\Lambda) \rightarrow A_1\alpha(k=\Lambda) + A_2$.

V. CONCLUSIONS

On the basis of the stability investigation around the UV and the IR fixed point one might attempt to sketch the global RG-flow. If one starts from the neighbourhood of the strongly coupled stable fixed point (24) one enters unavoidably into the subspace of composite couplings and at the same time the projection of the RG-flow into the subspace of local 4-fermion couplings evolves towards the Gaussian point. After passing the mass scale of the composite spectra the composite couplings enter a scaling regime. The direct four-fermion interaction is washed out from the system, and a weakly interacting bosonic field theory represents the symmetric phase of the NJL model at the longest wavelengths.

The main new result of the present investigation is to provide a numerical method to extract the interaction energy of the two particles as function of the initial physical size of the composite they constitute. For this we solved the renormalisation group equations derived from an ansatz for the effective quantum action with physically motivated parametrisation.

It is important to emphasize that by varying the initial width-parameter $\alpha(0)$ in the RG-equations we could explore a continuously infinite set of the approximate two-particle eigenmodes of the 4-fermion function of the original model. The resulting squared mass for any single solution in itself was not sufficient to decide whether one deals with a bound-state or only a component of the continuum. Only, by considering the complete set, we were able to single out the state with maximally negative interaction energy, and suggest a bound state interpretation for it. This way of processing is a fully consistent (though approximate) realisation of the strategy which emerged from our general discussion in Ref.[24].

APPENDIX

The renormalisation group equations are written for the dimensionless couplings

$$\mu_C^2 = \frac{M_C^2}{Z_C k^2}, \quad \tilde{g}_{Cr}^2 = \frac{g_C^2 e^{-2\alpha Q^2}}{Z_\psi^2 Z_C}, \quad \alpha_r = \alpha k^2, \quad \lambda_r = \frac{\lambda}{Z_C^2}, \quad \delta\lambda_{\sigma r} = \frac{k^2 \delta\lambda_\sigma}{Z_\psi^2}, \quad \lambda_{Vr} = \frac{k^2 \lambda_V}{Z_\psi^2}. \quad (40)$$

The dimensionful quantities are reconstructed by the formulae:

$$M_{phys}^2(t) = \mu_C^2(t) e^{2t} e^{-\eta_C(t)} \Lambda^2, \quad \alpha_{phys} = \alpha_r(t) e^{-2t} \frac{1}{\Lambda^2}, \quad (41)$$

where Λ is the scale where the solution of the RG-equations is starting. The explicit equations were derived using an optimized regulator [29].

The RG-equations of scaled four fermion couplings λ_{Vr} and $\delta\lambda_{\sigma r}$ contain terms which coincide with those appearing in the RGE's of the chiral NJL-model [28]. In addition two more contributions come when evaluating (19) and (20):

$$\begin{aligned} \partial_t \delta\lambda_{\sigma r} &= 2(1 + \eta_\psi) \delta\lambda_{\sigma r} - \frac{1}{8\pi^2} (\delta\lambda_{\sigma r}^2 + 4\delta\lambda_{\sigma r} \lambda_{Vr} + 3\lambda_{Vr}^2) \\ &+ \frac{\tilde{g}_{Cr}^4}{16\pi^2} [(2 - \eta_C) F_1(8\alpha_r) + \eta_C F_2(8\alpha_r)] \frac{1}{(1 + \mu_C^2)^3} \\ &+ \frac{\tilde{g}_{Cr}^4}{16\pi^2} [(1 - \eta_\psi) F_1(8\alpha_r) + \eta_\psi H_2(8\alpha_r)] \frac{1}{(1 + \mu_C^2)^2} \\ &+ \frac{\tilde{g}_{Cr}^2}{16\pi^2} (\delta\lambda_S - \lambda_V) [(2 - \eta_C) F_1(4\alpha_r) + \eta_C F_2(4\alpha_r)] \frac{1}{(1 + \mu_C^2)^2}, \\ \partial_t \lambda_{Vr} &= 2(1 + \eta_\psi) \lambda_{Vr} - \frac{1}{16\pi^2} (\delta\lambda_{\sigma r}^2 + 2\delta\lambda_{\sigma r} \lambda_{Vr} + \lambda_{Vr}^2) \\ &+ \frac{\tilde{g}_{Cr}^4}{16\pi^2} [(2 - \eta_C) F_1(8\alpha_r) + \eta_C F_2(8\alpha_r)] \frac{1}{(1 + \mu_C^2)^3} \\ &+ \frac{\tilde{g}_{Cr}^4}{16\pi^2} [(1 - \eta_\psi) F_1(8\alpha_r) + \eta_\psi H_2(8\alpha_r)] \frac{1}{(1 + \mu_C^2)^2}, \\ &+ \frac{\tilde{g}_{Cr}^2}{16\pi^2} (\delta\lambda_S + \lambda_V) [(2 - \eta_C) F_1(4\alpha_r) + \eta_C F_2(4\alpha_r)] \frac{1}{(1 + \mu_C^2)^2}. \end{aligned} \quad (42)$$

The amplitude of the bound state "wave function" figures in the equations always in the combination $\tilde{g}_{Cr} = g_{Cr} \exp(-2\alpha_r Q_r^2)$. The corresponding RG-equations read:

$$\begin{aligned} \partial_t \tilde{g}_{Cr}^2 &= (2\eta_\psi + \eta_C) \tilde{g}_{Cr}^2 - (\delta\lambda_{\sigma r} + \lambda_{Vr}) \tilde{g}_{Cr}^2 \frac{2}{\pi^2} [F_1(4\alpha_r)(1 - \eta_\psi) + H_2(4\alpha_r)\eta_\psi], \\ \partial_t (\tilde{g}_{Cr} \alpha_r (2 - \alpha_r Q_r^2)) &= \left(\eta_\psi + \frac{1}{2} \eta_C + 2 \right) \tilde{g}_{Cr} \alpha_r (2 - \alpha_r Q_r^2) \\ &- \frac{\tilde{g}_{Cr} (\delta\lambda_{\sigma r} + \lambda_{Vr})}{4\pi^2} \left\{ \frac{1}{2} e^{-4\alpha_r} - 16\alpha_r^2 [(1 - \eta_\psi) F_2(4\alpha_r) + \eta_\psi H_3(4\alpha_r)] \right. \\ &\quad \left. + 4\alpha_r (4 - \alpha_r Q_r^2) [(1 - \eta_\psi) F_1(4\alpha_r) + \eta_\psi H_2(4\alpha_r)] + 3 [(1 - \eta_\psi) F_0(4\alpha_r) + \eta_\psi H_1(4\alpha_r)] \right\}. \end{aligned} \quad (43)$$

Here the functions $F_n(\kappa)$ and $H_n(\kappa)$ are explicit weighted phase space integrals:

$$F_n(\kappa) = \int_0^1 dy y^{2n+1} e^{-\kappa y^2} = \frac{1}{2} \left(-\frac{d}{d\kappa} \right)^n \frac{1 - e^{-\kappa}}{\kappa}, \quad H_n(\kappa) = \int_0^1 dy y^{2n} e^{-\kappa y^2}. \quad (44)$$

Finally, the couplings describing the effective potential of the composite field obey the following equations:

$$\partial_t \mu_C^2 = -(2 - \eta_C) \mu_C^2 + \frac{\tilde{g}_{Cr}^2}{\pi^2} [(1 - \eta_\psi) F_1(8\alpha_r) + \eta_\psi H_2(8\alpha_r)] - \frac{\lambda_r}{24\pi^2} \frac{1}{(1 + \mu_C^2)^2} \left(1 - \frac{\eta_C}{6} \right), \quad (45)$$

$$\partial_t \lambda_r = 2\eta_C \lambda_r + \frac{5\lambda_r^2}{24\pi^2} \frac{1}{(1+\mu_C^2)^3} \left(1 - \frac{\eta_C}{6}\right) - \frac{12\tilde{g}_{Cr}^4}{\pi^2} [(1-\eta_\psi)F_1(16\alpha_r) + \eta_\psi H_2(16\alpha_r)]. \quad (46)$$

The expressions of the anomalous field dimensions are given with the expressions:

$$\begin{aligned} \eta_\psi &= \frac{\tilde{g}_{Cr}^2}{8\pi^2} \frac{1}{(1+\mu_C^2)^2} \left[(2-\eta_C) \left(\frac{3}{4} H_1(4\alpha_r) - 2\alpha_r H_2(4\alpha_r) \right) + \eta_C \left(\frac{3}{4} H_2(4\alpha_r) - 2\alpha_r H_3(4\alpha_r) \right) \right], \\ \eta_C &= \frac{\tilde{g}_{Cr}^2}{8\pi^2} \left(\frac{1}{2} e^{-8\alpha_r} - (1-\eta_\psi) [64\alpha_r^2 F_2(8\alpha_r) - 32\alpha_r F_1(8\alpha_r) - 3F_0(8\alpha_r)] \right. \\ &\quad \left. - \eta_\psi [64\alpha_r^2 H_3(8\alpha_r) - 32\alpha_r H_2(8\alpha_r) - 3H_1(8\alpha_r)] \right). \end{aligned} \quad (47)$$

ACKNOWLEDGEMENT

This research was supported by the Hungarian Research Fund under the contract K104292.

-
- [1] G. Panico and A. Wulzer, *The composite Nambu-Goldstone Higgs*, Lecture Notes in Physics, vol. **913**, Springer Int. Publ., 2016, ISBN 978-3-319-22616-3
 - [2] Z. Fodor and C. Hoelbling, Rev. Mod. Phys. **84** (2012) 449
 - [3] C.B. Lang, AIP Conf. Proc. **1735** (2016) 020002
 - [4] J. Kuti, PoS(Lattice2013)005; O. Witzel PoS(Lattice 2018) arXiv:1901.08216
 - [5] H. Bethe and E.E. Salpeter, Phys. Rev. **82** (1951) 309
 - [6] E.E. Salpeter and H. Bethe, Phys. Rev. **84** (1951) 1232
 - [7] P. Maris, C.D. Roberts and P. Tandy, Phys. Lett. B **420** (1998) 267
 - [8] G. Eichmann, A. Krassnigg, M. Schwinzerl, and R. Alkofer, Annals Phys. **323**, 2505 (2008)
 - [9] A. Krassnigg, Phys. Rev. D **80** (2009) 114010
 - [10] G. Eichmann, H. Sanchis-Alepuz, R. Williams, R. Alkofer, C.S. Fischer, Prog. Part. Nucl. Phys. **91**, 1 (2016)
 - [11] C. Wetterich, Phys. Lett. B **301** (1993) 90
 - [12] T.R. Morris, Int. J. Mod. Phys. A **9** (1994) 2411
 - [13] U. Ellwanger, Z. f. Physik C **62** (1994) 503
 - [14] U. Ellwanger and C. Wetterich, Nucl. Phys. B **423** (1994) 137
 - [15] H. Gies and C. Wetterich, Phys. Rev. D **65** (2002) 065001
 - [16] Stratonovich, R.L. Soviet Physics Doklady. **2**(1958) 416,
 - [17] J. Hubbard, J. Phys. Rev. Lett. **3** (1959) 77.
 - [18] S. Floerchinger and C. Wetterich, Phys. Lett. B **680** (2009) 371
 - [19] J.M. Pawłowski, Ann. Phys. (N.Y.) **322** (2007) 2831
 - [20] A.K. Cyrol, M. Mitter, J.M. Pawłowski and N. Strodthoff, Phys. Rev. D **97** (2018) 054006
 - [21] M. Mitter, J.M. Pawłowski and N. Strodthoff, Phys. Rev. D **91** (2015) 054035
 - [22] J. Braun, L. Fister, J.M. Pawłowski and F. Rennecke, Phys. Rev. D **93** (2016) 034016
 - [23] R. Alkofer, A. Maas, W.A. Mian, M. Mitter, J. Paris-Lopez, J.M. Pawłowski and N. Wink, arXiv:1810.07955
 - [24] A. Jakovác and A. Patkós, *Bound states in Functional Renormalisation Group* arXiv:1811.09418
 - [25] A. Jakovác, A. Patkós, Zs. Szép and P. Szépfalusy, Phys. Lett. B **582** (2004) 179
 - [26] P. Kovács and Zs. Szép, Phys. Rev. D **75** (2007) 025015
 - [27] P. Kovács and Zs. Szép, Phys. Rev. D **77** (2008) 065016
 - [28] J. Braun, J. Phys. G **39** (2012) 033001
 - [29] D. Litim, Phys. Rev. D **64**, 105004 (2001)
 - [30] J. Braun, M. Leonhardt, and M. Pospiech, Phys. Rev. D **96** (2017) 076003